Inhibition of the Na$^+$/dicarboxylate cotransporter

by anthranilic acid derivatives.

Ana M. Pajor and Kathleen M. Randolph

Department of Biochemistry and Molecular Biology,

University of Texas Medical Branch, Galveston, TX 77555-0645

Running title: Inhibitor binding in NaDC1

Corresponding author: Ana M. Pajor, Ph.D., Department of Biochemistry and Molecular Biology, University of Texas Medical Branch, Galveston, TX 77555-0645. tel. 409-772-3434, fax 409-772-5102, email: ampajor@utmb.edu

Document statistics:

Number of:

	text pages	12
	tables	1
	figures	11
	references	26

Number of words in:

Abstract	216
Introduction	474
Discussion	976

Nonstandard abbreviations: AACOCF$_3$, arachidonyl trifluoromethyl ketone; ACA, N-(p-amylcinnamoyl) anthranilic acid; BPB, p-bromophenacyl bromide; CUBS cell line, HRPE cells stably transfected with hNaDC1; DMSO, dimethylsulfoxide; Fmoc-anthranilic acid, N-(9-fluorenylmethoxycarbonyl)-anthranilic acid; HRPE, cell line derived from human embryonic retinal pigment epithelium; NaDC1, Na$^+$/dicarboxylate cotransporter 1; ONO-RS-082, 2-(p-amylcinnamoyl)amino-4-chloro benzoic acid; Tranilast, N-(3',4'-dimethoxycinnamoyl) anthranilic acid

ABSTRACT

The Na$^+$/dicarboxylate cotransporter NaDC1 absorbs citric acid cycle intermediates from the lumen of the small intestine and kidney proximal tubule. No effective inhibitor has been identified yet, although previous studies showed that the non-steroidal anti-inflammatory drug, flufenamate, inhibits the human (h) NaDC1 with an IC_{50} of 2 mM. In the present study, we have tested compounds related in structure to flufenamate, all anthranilic acid derivatives, as potential inhibitors of hNaDC1. We find that N-(p-amylcinnamoyl) anthranilic acid (ACA) and 2-(p-amylcinnamoyl)amino-4-chloro benzoic acid (ONO-RS-082) are the most potent inhibitors with IC_{50} values below 15 μM, followed by N-(9-fluorenylmethoxycarbonyl)-anthranilic acid (Fmoc-anthranilic acid) with an IC_{50} ~80 μM. The effects of ACA on NaDC1 are not mediated through a change in transporter protein abundance on the plasma membrane and appear to be independent of its effect on phospholipase A$_2$ activity. ACA acts as a slow inhibitor of NaDC1, with slow onset and slow reversibility. Both uptake activity and efflux are inhibited by ACA. Other Na$^+$/dicarboxylate transporters from the SLC13 family, including hNaDC3 and rbNaDC1, were also inhibited by ACA, ONO-RS-082 and Fmoc-anthranilic acid, whereas the Na$^+$/citrate transporter (hNaCT) is much less sensitive to these compounds. The endogenous sodium-dependent succinate transport in Caco-2 cells is also inhibited by ACA. In conclusion, ACA and ONO-RS-082 represent promising lead compounds for the development of specific inhibitors of the Na$^+$/dicarboxylate cotransporters.

Introduction

The metabolic intermediates of the citric acid cycle, including succinate, citrate and α-ketoglutarate, are transported across the plasma membranes of epithelial cells by the

Na$^+$/dicarboxylate cotransporters from the SLC13 family (Pajor, 2006). SLC13 family members include the low affinity dicarboxylate transporter, NaDC1, the high affinity Na$^+$/dicarboxylate cotransporter, NaDC3, and the Na$^+$/citrate transporter, NaCT. NaDC1 is found on the apical membranes of renal proximal tubule and small intestinal cells. In the kidney, NaDC1 helps to regulate the concentration of citrate in the urine, which is an important determinant in the development of kidney stones, as ~ 50% of patients with kidney stones have hypocitraturia (Pak, 1991). NaDC1 also participates in organic anion secretion in the kidney by providing dicarboxylate substrates, particularly α-ketoglutarate, to the organic anion transporter of the basolateral membrane (Dantzler and Evans, 1996). NaDC1 may play an indirect role in regulating blood pressure, as succinate and α-ketoglutarate activate specific G-protein-coupled receptors in the renal proximal tubule (He et al., 2004). Finally, mutations in NaDC1 homologs found in the digestive tract of *Drosophila* and *C. elegans* lead to an extension of lifespan (Rogina et al., 2000;Fei et al., 2004) suggesting a possible role for NaDC1 in metabolic control or aging.

To date, no high-affinity inhibitors have been identified for any member of the SLC13 family. Our previous studies identified the non-steroidal anti-inflammatory drug flufenamate as an inhibitor of hNaDC1. The IC$_{50}$ was 2 mM using succinate as a substrate and 0.5 mM using methylsuccinate (Pajor and Sun, 1996;Smith et al., 2003). A high-affinity inhibitor would be very useful for *in vitro* studies of NaDC1, to quantitate the transporter in the membrane and to characterize mutant transporters with alterations in substrate translocation but not binding. An effective and selective inhibitor could help to identify physiological roles of NaDC1. Furthermore, an inhibitor may lead to a potential drug if inhibition of NaDC1 activity in humans is linked to aging or metabolism.

In the present study, we have tested anthranilic acid derivatives related in structure to flufenamate as potential inhibitors of hNaDC1. We find that N-(p-amylcinnamoyl) anthranilic acid (ACA) and 2-(p-amylcinnamoyl)amino-4-chloro benzoic acid (ONO-RS-082) are the most potent inhibitors with IC_{50} values below 15 μM, followed by N-(9-fluorenylmethoxycarbonyl)-anthranilic acid (Fmoc-anthranilic acid) with an IC_{50} ~80 μM. The effects of ACA on hNaDC1 are not mediated through a change in transporter protein abundance on the plasma membrane and appear to be independent of its effect on phospholipase A_2 (PLA_2) activity. ACA acts as a slow inhibitor of NaDC1, with slow onset and slow reversibility. Both transport uptake and efflux are inhibited by ACA. Other Na^+/dicarboxylate transporters from the SLC13 family, including hNaDC3 and rbNaDC1, were also inhibited by ACA, ONO-RS-082 and Fmoc-anthranilic acid, whereas the Na^+/citrate transporter hNaCT is much less sensitive to these compounds. The endogenous sodium-dependent succinate transport activity in the human colon carcinoma cell line, Caco-2, is also sensitive to inhibition by ACA. In conclusion, ACA and ONO-RS-082 are promising lead compounds for the development of specific inhibitors of the Na^+/dicarboxylate cotransporters.

Materials and Methods

Chemicals. The structures of the compounds used in this study are shown in Fig. 1 and the names are listed in Table 1. ACA, ONO-RS-082 and Tranilast were purchased from Biomol Research Laboratories, all other chemicals were from Sigma-Aldrich.

Cell culture. The CUBS cell line consisting of HRPE cells (derived from human retinal pigment epithelium) stably transfected with the human NaDC1 cDNA (Smith et al., 2003) was a generous gift of Dr. Chari Smith (GlaxoSmithKline). Control cells were non-transfected HRPE cells. Cells were cultured in Modified Eagle's Medium containing Earle's salts, Glutamax I and 25 mM HEPES (Gibco-BRL), supplemented with 10% heat-inactivated fetal calf serum (Hyclone), 100 units/ml penicillin and 100 μg/ml streptomycin and 700 μg/ml Geneticin (G418; Gibco-BRL) at 37°C in 5% CO_2. For uptake experiments, cells were plated on white-sided 24-well plastic Visiplates (PerkinElmer/Wallac) at a density of 2.5 x 10^5 cells per well (24-well plate) in the same medium with 2.5 mM buytrate added. Control HRPE cells were plated at the same density but without G418 or butyrate in the medium. Uptake assays were done in confluent monolayers approximately 36 hours after plating.

For transient transfections with hNaDC3 and hNaCT, HRPE cells were plated at 1.2 x 10^5 cells per well and each well of cells was transfected with 1.8 µl Fugene 6 (Roche) and 0.6 µg plasmid DNA (9:3 ratio) (Pajor and Randolph, 2005). Transport assays were done 48 hours after transfections.

Succinate uptake assay. Transport assays at room temperature were as described previously (Pajor and Randolph, 2005). The sodium buffer contained in mM: 120 NaCl, 5 KCl, 1.2 $MgCl_2$, 1.2 $CaCl_2$, 5 D-glucose, 25 HEPES, pH adjusted to 7.4 with 1 M Tris. Choline

buffer contained 120 mM choline chloride in place of NaCl.   For the assays, each well was washed twice with 1 ml sodium buffer, then pre-incubated with inhibitor in sodium buffer for 15 min, followed by two washes with 1 ml each sodium buffer. Inhibitors were prepared fresh each day as DMSO stocks, with a final volume of DMSO of less than 1%. Cells were preincubated with inhibitors 15 min (unless otherwise specified in the figure legends).   Transport solution (0.25 ml/well) consisting of [^{14}C]succinate (10 or 100 μM final concentration) in sodium buffer, with or without added inhibitor, was then added to the cells. After 30 minutes, the uptake measurements were stopped and radioactivity removed with four 1 ml washes of choline buffer. After the last wash was removed, each well of cells was dissolved in 0.5 ml scintillation cocktail, OptiPhase Supermix (Wallac/Perkin Elmer). The plates were sealed with plastic plate covers and counted directly in a Microbeta Trilux 1450 plate scintillation counter (Wallac/Perkin Elmer).   For experiments involving CUBS cells, background corrections were made based on uptake activities in control HRPE cells. For experiments involving transfected cells, uptake activities in vector-transfected cells were subtracted from activities in NaDC plasmid-transfected cells. There was no difference in the background counts obtained with vector-transfected or non-transfected cells (results not shown).

For calculation of K_i values from Dixon plots, inhibition of transport activity was measured at multiple inhibitor and substrate concentrations. The data were analyzed by linear regression and the x-axis value corresponding to the intersection of the lines was taken as -K_i (Segel, 1975). To determine IC$_{50}$ values (the inhibitor concentration resulting in 50% inhibition), the transport of 10 μM [^{14}C]succinate was measured in the presence of increasing concentrations of inhibitor and the resulting activity (v%, as a percentage of control) was analyzed by non-linear regression using v%= IC$_{50}$/([I] + IC$_{50}$) * 100, where [I] represents the inhibitor concentration. Statistical

7

analysis with One-way Anova or Student's *t*-test was done using the Sigma Stat program (Jandel). Each experimental point was the mean of four replicate wells, and each experiment was repeated at least two or three times (different plating or transfection experiments).

Efflux assays. Efflux assays in CUBS cells (Smith et al., 2003) were done using the non-metabolizable substrate, [^{3}H]methylsuccinate (a gift of Dr. Chari Smith, GlaxoSmithKline). In preliminary experiments (not shown) we found that the cells required at least 30 minutes of incubation with substrate for preloading, after which the intracellular radioactivity reached a plateau. Therefore, the cells were preloaded by incubating with 10 or 100 μM [^{3}H]methylsuccinate in Na$^+$ buffer for 30 minutes. The cells were then washed four times with choline buffer to remove extracellular radioactivity, followed by incubation in sodium buffer for one minute to allow efflux of radiolabeled substrate. To stop the efflux, each well was washed four times with choline buffer and 1% SDS was added to solubilize the cells. The samples were transferred to scintillation vials (since the Wallac Plate counter does not measure ^{3}H accurately), combined with scintillation cocktail and counted on a Packard Tri-Carb 2100TR scintillation counter.

Caco-2 cells. The Caco-2 cell line (human colon adenocarcinoma) was obtained from the American Type Culture Collection (Rockville, MD). The cells were cultured in DMEM with 4.5 g/l glucose (GIBCO-Invitrogen) supplemented with 10% heat-inactivated fetal calf serum (Hyclone), 100 units/ml penicillin G, 100 ug/ml streptomycin, 1% (v/v) sodium pyruvate and 1% (v/v) nonessential amino acids (Sigma). Cells were seeded in 24 well collagen-coated plates, maintained with medium changes every other day and then used for transport assays 21 days after reaching confluency. Sodium-dependent transport activity was the difference between transport measured in sodium and choline-containing buffers.

8

Cell surface biotinylation. Cell surface biotinylations of NaDC1 were done using a membrane impermeant reagent, Sulfo-NHS-LC-biotin, as described previously (Pajor and Randolph, 2005). Biotinylated proteins were separated by SDS-PAGE in 7.5% acrylamide and NaDC1 was identified using antibodies (1:1000 dilution).

Results

Initial inhibitor screen. The time course of [^{14}C]succinate uptake into the CUBS cell line (stably transfected HRPE cells expressing the human Na$^+$/dicarboxylate cotransporter, hNaDC1) is linear through 45 min (Fig. 2). Therefore, 30 min uptake activities were used in subsequent experiments as estimates of initial rates. Succinate uptake activity in control non-transfected HRPE cells was very low (Fig. 2). The transport of succinate in choline buffer in the CUBS cell line was the same as in non-transfected HRPE cells (results not shown).

Several commercially-available anthranilic acid derivatives were tested as potential inhibitors of NaDC1 (Fig. 3). CUBS cells expressing hNaDC1 were incubated with test inhibitors, each at 100 μM concentration, and the effect on succinate transport was measured. We found that ACA (compound 1) and the related compound ONO-RS-082 (compound 2) produced greater than 80% inhibition of succinate transport. Incubation with N-Fmoc-anthranilic acid (compound 4) resulted in approximately 45% inhibition. None of the other compounds produced significant inhibition at 100 μM concentration. There was also no inhibition of succinate transport by anthranilic acid, the parent compound (not shown). The lack

9

of inhibition by 100 μM flufenamate was consistent with the apparent IC_{50} value of 2 mM in hNaDC1 expressed in *Xenopus* oocytes (Pajor and Sun, 1996).

Kinetics of inhibition. The mechanism of inhibition of NaDC1 by ACA was examined using Dixon plots (Fig. 4). The lines intersected at the x-axis, suggesting that the mechanism of inhibition is non-competitive (Segel, 1975). In the experiment shown in Fig. 4, the K_i was 12.5 μM, and in four experiments the K_i was 15.3 ± 3.3 μM (mean +/- SEM). We also compared the IC_{50} values for the three inhibitory compounds, ACA, ONO-RS-082 and Fmoc-anthranilic acid, measured at a single substrate concentration (10 μM succinate). The IC_{50} values were 10.6 ± 2.4 μM (ACA), 9.2 ± 0.3 μM (ONO-RS-082) and 85.3 ± 13.3 μM (Fmoc-anthranilic acid), n=3 (results not shown).

Cell surface biotinylation. One possible explanation for the decrease in transport activity after ACA treatment is a decrease in the amount of transporter protein at the plasma membrane. This was tested by cell surface biotinylation using the membrane impermeant reagent, Sulfo-NHS-LC-biotin. Cells treated with ACA did not show any evidence of internalization of hNaDC1 protein compared with controls incubated with buffer for the same incubation period (Fig. 5). Therefore, the decreased activity seen after incubation with ACA is not due to internalization of the transporter.

Time courses of ACA inhibition. Several alternative explanations could account for the apparent non-competitive inhibition of hNaDC1 by ACA. For example, ACA could act as an irreversible inhibitor or a slow, reversible inhibitor, both of which would produce apparent non-competitive inhibition (Segel, 1975; Morrison, 1982). In time course experiments, the inhibition by ACA did not occur immediately and the inhibition was not evident until after 2 minutes of incubation (Fig. 6). A longer time course (Fig. 7A) shows that the inhibition by ACA requires

10

at least 15 to 30 minutes of preincubation. The inhibition also appeared to be reversible, although very slow. In one hour, the activity of hNaDC1 recovered by approximately 20% (Fig. 7B). The inhibition by ACA was not dependent on cations, since the extent of inhibition was the same in sodium or choline buffer. Transport activity remaining after pretreatment with 30 μM ACA was 66 ± 5% in sodium buffer compared with 71 ± 3.5% in choline buffer (n=3 experiments).

Efflux experiments. We next tested the efflux of the non-metabolizable substrate, [^{3}H]methylsuccinate, in the CUBS cell line. The cells were pre-loaded with radiolabled substrate in sodium buffer for 30 minutes. The extracellular radioactivity was washed away and the efflux was measured for 1 minute in sodium buffer with or without 100 μM ACA. As shown in Fig. 8, approximately 40-50% of the [^{3}H]methylsuccinate remained in the cells after 1 min compared to controls at time 0. The addition of 100 μM ACA resulted in an increased retention of [^{3}H]methylsuccinate during the efflux period (Fig. 8), indicating that efflux as well as influx is inhibited by ACA.

Phospholipase A$_2$ inhibitors. Since ACA is known to be a non-specific inhibitor of phospholipase A$_2$ (PLA$_2$) (Konrad et al., 1992), we wanted to rule out the possibility that the effects of ACA on NaDC1 are mediated indirectly by inhibition of PLA$_2$. Two other inhibitors of PLA$_2$, structurally unrelated to ACA, were tested but they did not inhibit succinate transport by hNaDC1 (Fig. 9). *p*-Bromophenacyl bromide (BPB) inhibits secreted PLA$_2$ by binding covalently to a histidine residue (Mayer and Marshall, 1993). A previous study showed that BPB at 5 or 10 μM inhibits PLA$_2$ activity in cultured cells without producing toxicity (Liu and Levy, 1997). AACOCF$_3$ (arachidonyl trifluoromethyl ketone) is a slow-onset inhibitor of the calcium-dependent cytosolic PLA$_2$ (Street et al., 1993). Both compounds were tested after 15

11

min preincubation time. The results suggest that the effects of ACA on hNaDC1 are distinct from its inhibition of PLA$_2$.

Species and isoform differences in specificity. We also examined the effects of the test inhibitors on transport activity of other SLC13 members, the high affinity Na$^+$/dicarboxylate cotransporter, hNaDC3 (Wang et al., 2000), the Na$^+$/citrate cotransporter, hNaCT (Inoue et al., 2002), and the rabbit (rb) NaDC1 (Pajor and Sun, 1996). The activity of hNaCT was tested using citrate as a substrate, whereas the substrate for hNaDC3 and rbNaDC1 was succinate. As shown in Fig. 10, the three transporters were sensitive to inhibition by some of the anthranilic acid derivatives. All three transporters were very sensitive to inhibition by ACA (compound 1), but in general, hNaCT was less sensitive to ONO-RS-082 (compound 2) and Fmoc-anthranilic acid (compound 4) compared with the other transporters. The rbNaDC1 was inhibited by flufenamate by ~40% (compound 10), whereas hNaDC3 and hNaCT were not affected by flufenamate. There was no inhibition of the three transporters by the other compounds (compound 11 shown in Fig. 10, other compounds not shown).

Inhibition of endogenous transporter. The human colon carcinoma cell line, Caco-2, is often used as a model of the small intestine. This cell line expresses sodium-dependent transport of succinate that is predominantly mediated by NaDC1, with some contribution by NaCT (Weerachayaphorn and Pajor, 2005). As shown in Fig. 11, the endogenous succinate transport activity in Caco-2 cells was inhibited more than 50% by treatment with ACA. Therefore, ACA inhibits both transfected recombinant NaDC1 and the endogenous NaDC1 found in Caco-2 cells.

Discussion

The main finding of this study is that anthranilic acid derivatives, including ACA, ONO-RS-082, and Fmoc-anthranilic acid, are inhibitors of the Na^{+}/dicarboxylate cotransporters from the SLC13 family. ACA and ONO-RS-082 inhibit transport with IC_{50} values less than 15 μM and thus represent the highest affinity inhibitors of hNaDC1 to date. The effects of ACA are not mediated through internalization of the transporter and appear to be distinct from the effects of ACA on phospholipase A_2. The preferred structure for inhibition of hNaDC1 appears to require a lipophilic moiety attached to the anthranilic acid moiety of the compound, since Fmoc-anthranilic acid (compound 4) was a more effective inhibitor compared with Tranilast (compound 3) or the compounds with smaller or more polar substituents.

Flufenamate was identified in previous studies as a low affinity inhibitor of both low affinity (NaDC1) and high affinity (NaDC3) Na^{+}/dicarboxylate cotransporters. There are species differences in sensitivity to flufenamate, with rbNaDC1 being most sensitive, IC_{50} 250 μM (Pajor and Sun, 1996), followed by flounder NaDC3 with an IC_{50} ~1mM (Burckhardt et al., 2004), and lastly hNaDC1, IC_{50} 2 mM (Pajor and Sun, 1996). All of the experiments were done using *Xenopus* oocytes as an expression system and the cells were not preincubated with inhibitor. In the present study, the IC_{50} for flufenamate in rbNaDC1 was ~ 100 μM, and the cells were preincubated with inhibitor before the assay, which may account for the apparent difference in affinity. Inhibition of the flounder NaDC3 by flufenamate appears to be mediated, at least in part, by an increased K^{+} conductance that is associated with the transporter, since it was not seen in control oocytes (Burckhardt et al., 2004). It is possible that flufenamate activates a channel activity of the fNaDC3 protein, and several members of the SLC13 family have both channel and transport activity (Oshiro and Pajor, 2005).

13

The onset of inhibition of hNaDC1 by ACA was not evident until after at least 2 min incubation time, consistent with the properties of a slow-binding inhibitor. This is the first report that ACA behaves as a slow-binding inhibitor. Slow-binding inhibitors are reversible, competitive inhibitors but the rate of reaching equilibrium is slow relative to a classical inhibitor (Morrison, 1982). Slow inhibition may occur if the formation of the enzyme-inhibitor complex occurs more slowly than the production of reaction product (in the case of a transporter, the "product" of the reaction is the appearance of substrate on the inside of the cell). Alternatively, the enzyme and inhibitor complex forms quickly but there is a slow isomerization step to an inactive complex. Slow inhibitors tend to be useful drugs because of their slow reversibility and the gradual accumulation of the inactive enzyme-inhibitor complex. Examples of drugs that are slow inhibitors include non-steroidal anti-inflammatory drugs (NSAIDS), such as indomethacin, that inhibit prostaglandin H synthase I by slow, reversible isomerization to a second enzyme-inhibitor complex (Callan et al., 1996). The arachidonic acid analog, AACOCF$_3$, is a slow and tight-binding inhibitor of the cytosolic phospholipase A$_2$ (Street et al., 1993).

Our current working hypothesis for the effects of the inhibitors identified in the present study is that they act directly on hNaDC1 to inhibit transport. Other hypotheses could also explain the results but they can be ruled out. For example, ACA could inhibit transport by affecting protein targeting. Both ACA (IC$_{50}$ 8 μM) and ONO-RS-082 (IC$_{50}$ 6 μM) have been shown to disrupt Golgi trafficking (de Figueiredo et al., 1999). However, the cell surface abundance of hNaDC1 was not affected by incubation with ACA. A second possible explanation is that ACA inhibits transport indirectly by affecting the membrane potential or Na$^+$ chemical gradient, which would affect hNaDC1 since it is electrogenic (Yao and Pajor, 2000).

ONO-RS-082 has been shown to inhibit the H^+/K^+-ATPase in stomach with an IC_{50} of 3.5 μM, and the same study also reported that ONO-RS-082 has a protonophore effect (Sugita et al., 2005). ACA is known to directly inhibit transient receptor potential (TRP) cation channels with an IC_{50} of less than 4 μM (Kraft et al., 2006). However, changes in membrane potential or cation concentrations would not explain the time delay in the inhibition of hNaDC1 by ACA, nor would it explain the different sensitivities of NaDC1 homologs, all of which are electrogenic.

The hypothesis that ACA inhibition is mediated indirectly through its inhibition of PLA_2 is less likely than a direct effect of ACA on hNaDC1. There was no inhibition of hNaDC1 activity by two structurally unrelated PLA_2 inhibitors, BPB and $AACOCF_3$. A compound that has not been reported to have PLA_2 inhibitory activity, Fmoc-anthranilic acid (compound 4), also inhibited transport with an IC_{50} of about 80 μM. Although flufenamate has been shown to inhibit PLA_2 (Franson et al., 1980), only the rabbit and not the human NaDC1 was inhibited by flufenamate. Furthermore, meclofenamate (compound 11) is also a PLA_2 inhibitor with an IC_{50} ~ 1 μM at 1 mM Ca^{2+} (Franson et al., 1980), yet it had no effect on any of the transporters in this study.

In conclusion, we have identified several inhibitors of the Na^+/dicarboxylate cotransporters, with micromolar affinities, that represent the highest affinity inhibitors of the SLC13 family to date. The most potent inhibitors of hNaDC1 were ACA, ONO-RS-082 and Fmoc-anthranilic acid. There were some differences in sensitivity to inhibition by anthranilic acid derivatives among the NaDC1 homologs tested (hNaDC3, rbNaDC1 and hNaCT), although the selectivity of the compounds was relatively low. The endogenous sodium-dependent succinate transport activity in the human colon carcinoma cell line, Caco-2, is also sensitive to inhibition by ACA.

The kinetics of ACA inhibition of hNaDC1 were consistent with slow inhibition, and both uptake and efflux were affected. Our data indicate that ACA inhibits the activity of hNaDC1 independently of PLA_2 inhibition. However, the lack of specificity of ACA and ONO-RS-082 with NaDC orthologs and the effects on other targets including PLA_2, TRP cation channels (Kraft et al., 2006) and the stomach H^+/K^+-ATPase (Sugita et al., 2005) would limit the use of these compounds as NaDC1 inhibitors. Therefore, the structures of the anthranilic acid derivatives will serve as a starting point in drug design targeting hNaDC1.

References

Burckhardt BC, Lorenz J, Burckhardt G and Steffgen J (2004) Interactions of benzylpenicillin and non-steroidal anti-inflammatory drugs with the sodium-dependent dicarboxylate transporter NaDC-3. *Cell Physiol Biochem* **14**:415-424.

Callan OH, So O Y and Swinney D C (1996) The kinetic factors that determine the affinity and selectivity for slow binding inhibition of human prostaglandin H synthase 1 and 2 by indomethacin and flurbiprofen. *J Biol Chem* **271**:3548-3554.

Dantzler WH and Evans K K (1996) Effect of αKG in lumen on PAH Transport by isolated perfused proximal tubules. *Am J Physiol* **271**:F521-F526.

de Figueiredo P, Polizotto R S, Drecktrah D and Brown W J (1999) Membrane tubule-mediated reassembly and maintenance of the golgi complex is disrupted by phospholipase A_2 antagonists. *Mol Biol Cell* **10**:1763-1782.

Fei YJ, Liu J C, Inoue K, Zhuang L, Miyake K, Miyauchi S and Ganapathy V (2004) Relevance of NAC-2, an Na^+-coupled citrate transporter, to life span, body size and fat content in *Caenorhabditis elegans*. *Biochem J* **379**:191-198.

Franson RC, Eisen D, Jesse R and Lanni C (1980) Inhibition of Highly purified mammalian phospholipases A_2 by non-steroidal anti-inflammatory agents. Modulation by calcium ions. *Biochem J* **186**:633-636.

He W, Miao F J P, Lin D C H, Schwander R T, Wang Z, Gao J, Chen J.L., Tian H and Ling L (2004) Citric acid cycle intermediates as ligands for orphan G-protein-coupled receptors. *Nature* **429**:188-193.

Inoue K, Zhuang L and Ganapathy V (2002) Human Na^+ -coupled citrate transporter: primary structure, genomic organization, and transport function. *Biochem Biophys Res Commun* **299**:465-471.

Konrad RJ, Jolly Y C, Major C and Wolf B A (1992) Inhibition of phospholipase A_2 and insulin secretion in pancreatic islets. *Biochim Biophys Acta* **1135**:215-220.

Kraft R, Grimm C, Frenzel H and Harteneck C (2006) Inhibition of TRPM2 cation channels by N-(p-amylcinnamoyl)anthranilic Acid. *Br J Pharmacol* **148**:264-273.

Liu Y and Levy R (1997) Phospholipase A2 has a role in proliferation but not in differentiation of HL-60 cells. *Biochim Biophys Acta* **1355**:270-280.

Mayer RJ and Marshall L A (1993) New insights on mammalian phospholipase A_2(s); comparison of arachidonoyl-selective and -nonselective enzymes. *FASEB J* **7**:339-348.

Morrison, J. F. The slow-binding and slow, tight-binding inhibition of enzyme-catalysed reactions. TIBS 7[3], 102-105. 1982.

Oshiro N and Pajor A M (2005) Functional characterization of high-affinity Na^+/dicarboxylate cotransporter found in *Xenopus laevis* kidney and heart. *Am J Physiol Cell Physiol* **289**:C1159-C1168.

Pajor AM (2006) Molecular properties of the SLC13 family of dicarboxylate and sulfate transporters. *Pflugers Arch* **451**:597-605.

Pajor AM and Randolph K M (2005) Conformationally sensitive residues in extracellular loop 5 of the Na^+/dicarboxylate co-transporter. *J Biol Chem* **280**:18728-18735.

Pajor AM and Sun N (1996) Functional differences between rabbit and human Na$^+$-dicarboxylate cotransporters, NaDC-1 and hNaDC-1. *Am J Physiol Renal Fluid Electrolyte Physiol* **271**:F1093-F1099.

Pak CYC (1991) Etiology and treatment of urolithiasis. *Am J Kidney Diseases* **18**:624-637.

Rogina B, Reenan R A, Nilsen S P and Helfand S L (2000) Extended life-span conferred by cotransporter gene mutations in *Drosophila*. *Science* **290**:2137-2140.

Segel IH (1975) *Enzyme Kinetics*. John Wiley and Sons, NY.

Smith, C., McCoy, D. Vaughan M., Pajor, A. M., Kerner, S., and Witherspoon, S. (2003) Functional expression and molecular pharmacology of hNaDC1. FASEB J. 17 (Abstract 331.13).

Street IP, Lin H K, Laliberte F, Ghomashchi F, Wang Z, Perrier H, Tremblay N M, Huang Z, Weech P K and Gelb M H (1993) Slow- and tight-binding inhibitors of the 85-KDa human phospholipase A$_2$. *Biochemistry* **32**:5935-5940.

Sugita Y, Nagao T and Urushidani T (2005) Nonspecific effects of the pharmacological probes commonly used to analyze signal transduction in rabbit parietal cells. *Eur J Pharmacol* **365**:77-89.

Wang H, Fei Y J, Kekuda R, Yang-Feng T L, Devoe L D, Leibach F H, Prasad P D and Ganapathy M E (2000) Structure, function and genomic organization of human Na$^+$-dependent high-affinity dicarboxylate transporter. *Am J Physiol Cell Physiol* **278**:C1019-C1030.

Weerachayaphorn, J., and Pajor, A.M. (2005) Na$^+$-dependent and –independent transport of succinate and citrate in the Caco-2 cell line. FASEB J 19 (4): A748 (Abstract)

Yao X. and Pajor A.M. (2000) The transport properties of the human renal Na^+-dicarboxylate

cotransporter under voltage-clamp conditions. *Am. J. Physiol. Renal Physiol*. **279**:F54-F64.

Figure Legends

Fig. 1 Structures of the compounds used in this study. The names of the compounds are listed in Table 1.

Fig. 2 Time course of [^{14}C]succinate transport (10 μM) in the CUBS cell line (HRPE cells stably expressing hNaDC1) compared with control HRPE cells. Each point represents the mean ± range of two wells from a single representative experiment.

Fig. 3 Inhibition of 10 μM [^{14}C]succinate transport by anthranilic acid derivatives in hNaDC1 expressed in CUBS cells. The numbers refer to different compounds as described in Table 1 and Fig.1. The test inhibitor concentrations were 100 μM. Thirty minute uptake measurements were done and the data are expressed as a percentage of control in the absence of inhibitor. The data points represent mean ± range or SEM, n=2-3 experiments. The * denotes significant difference from control, $p < 0.05$.

Fig. 4 Dixon plots of ACA inhibition of hNaDC1 in the CUBS cell line. Transport assays were done in 24 well plates at two different [^{14}C]succinate concentrations (10 and 100 μM) and increasing amounts of ACA. The data points represent mean ± SEM, n=4 wells, from a single representative experiment. The K_i in this experiment is 12.5 μM.

Fig. 5 Western blot of cell surface biotinylated hNaDC1 in the CUBS cell line. Cells were incubated with sodium buffer with or without 25 μM ACA for 20 min. The cell surface proteins were labeled with the membrane impermeant reagent, Sulfo-NHS-LC-biotin, as described in Methods. Western blots of biotinylated proteins were probed with anti-

21

NaDC1 antibodies (1:1000 dilution) followed by horseradish peroxidase linked anti-rabbit immunoglobulin (1:5000 dilution). The chemiluminescent size standards (Magic Mark) are shown in lane 1.

Fig. 6   Time course of inhibition by ACA.   Transport of 10 μM [^{14}C]succinate by hNaDC1 in the CUBS cell line was measured in the absence (control) or presence (+ACA) of 50 μM ACA. Datapoints represent means ± range of duplicate measurements, some error bars are smaller than the points.

Fig. 7 Time courses of ACA preincubation and postincubation with hNaDC1 in the CUBS cell line. **A. Onset**. The cells were preincubated with or without 50 μM ACA in sodium buffer for up to 30 minutes, then transport of [^{14}C]succinate was assayed for 30 minutes. Data are expressed as a percentage of control at each time point (parallel incubation in the absence of ACA). **B. Reversibility**. The cells were incubated with 30 μM ACA for 15 minutes, the ACA was washed away and the cells were then incubated in sodium buffer for up to 60 minutes. Control cells were incubated with sodium buffer only. Transport of 10 μM [^{14}C]succinate was measured for 30 min.   Data shown are means ± SEM, n=4 wells.

Fig. 8   Effect of ACA on efflux.   CUBS cells expressing hNaDC1 were preloaded by incubating with [^{3}H]methylsuccinate (10 or 100 μM) for 30 minutes. The extracellular radioactivity was washed away and the cells were then incubated with sodium buffer alone (control) or with 100 μM ACA (+ ACA) for 1 minute. The data shown are the means ± SEM, n=4 experiments, * significantly different from control group, p < 0.05.

Fig. 9 Effect of phospholipase A_2 inhibitors on [^{14}C]succinate transport by hNaDC1 in CUBS cells. The inhibitors, p-bromophenacyl bromide (BPB) and arachidonyl trifluoromethyl ketone (AACOCF$_3$), were applied at 10 μM for a 15 min preincubation followed by co-incubation with [^{14}C]succinate during the 30 min uptake period. Control cells were incubated in sodium buffer without inhibitor.   Data are means ± range of duplicate experiments.

Fig. 10 Sensitivity of the high affinity Na$^+$/dicarboxylate cotransporter, hNaDC3, the Na$^+$/citrate cotransporter, hNaCT, and the low-affinity Na$^+$/dicarboxylate cotransporter, rbNaDC1 to inhibition by anthranilic acid derivatives. Compound names are listed in Table 1, structures are shown in Fig. 1.   HRPE cells were transiently transfected with plasmids containing transporter cDNA, control cells were transfected with the pcDNA3.1 vector plasmid.   Transport of 10 μM [^{14}C]succinate (hNaDC3, rbNaDC1) or [^{14}C]citrate (hNaCT) was measured for 30 min in the presence or absence of 100 μM inhibitor. Data shown are means ± range or SEM, n=2-3 experiments, except for rbNaDC1 with compound 11 (n=1).

Fig. 11 Endogenous sodium-dependent succinate transport in Caco-2 cells treated with or without 50 μM ACA. Caco2 cell monolayers were grown 21 days after reaching confluence. The cells were pre-incubated 15 min with ACA or sodium buffer alone and then transport of 100 μM [^{14}C]succinate was measured in sodium or choline buffer for 30 min.   Data shown are means ± SEM, n=3 experiments. The * denotes significant difference from control, p<0.05.

TABLE 1: List of compounds used in this study. The numbers refer to the structures shown in Fig. 1.

Number	Name
1	ACA, N-(p-amylcinnamoyl)anthranilic acid
2	ONO-RS-082, N-(p-amylcinnamoyl) amino-4-chloro anthranilic acid
3	Tranilast, N-(3',4'-dimethoxycinnamoyl)anthranilic acid
4	N-Fmoc-anthranilic acid, N-(9-fluorenylmethoxycarbonyl)-anthranilic acid
5	N-(2-cyanoacetyl) anthranilic acid
6	5-chloro-N-(2-chloroacetyl)anthranilic acid
7	5-bromo-N-(barboxymethyl)anthranilic acid
8	N-(acetoacetyl) anthranilic acid
9	N-(4-nitrobenzoyl) anthranilic acid
10	Flufenamate, N-(3-trifluoromethylphenyl) anthranilic acid
11	Meclofenamate, 2-[(2,6-dichloro-3-methylphenyl)amino]benzoic acid
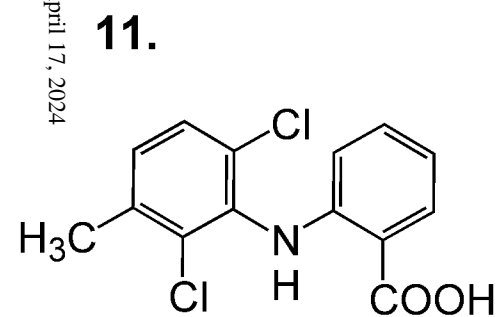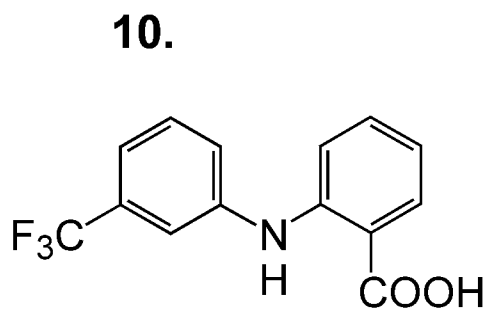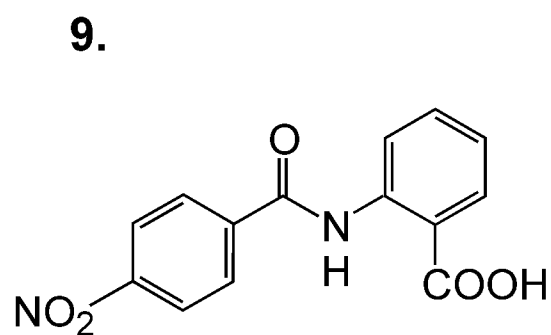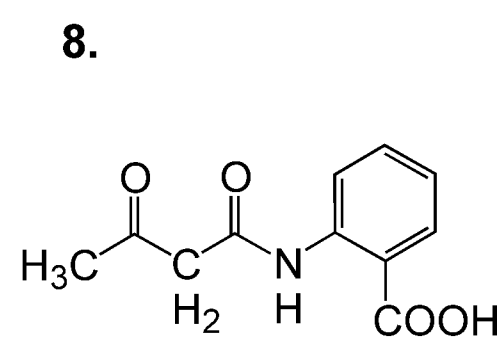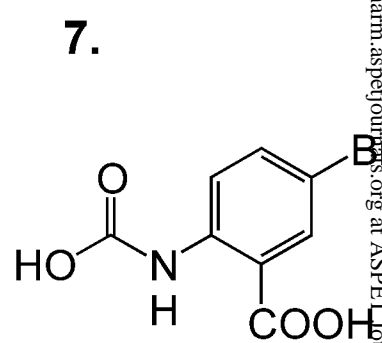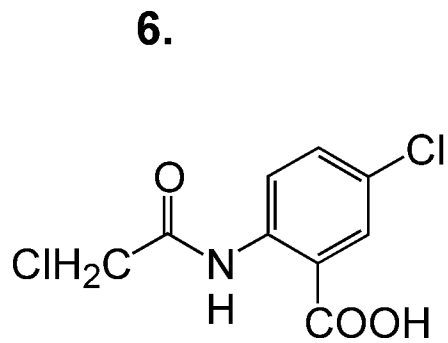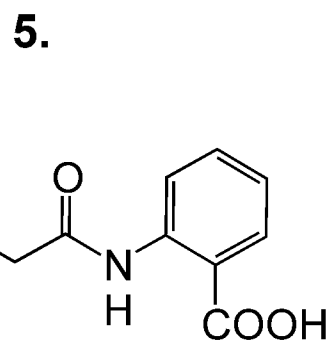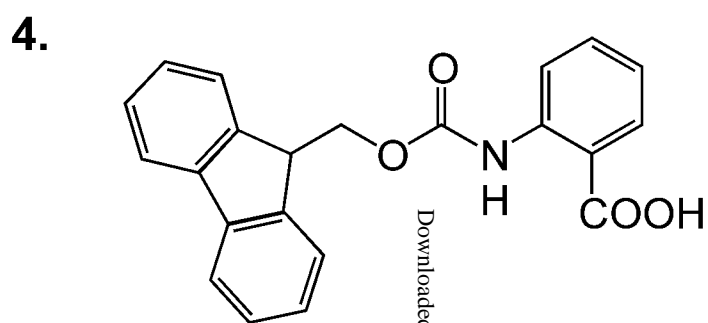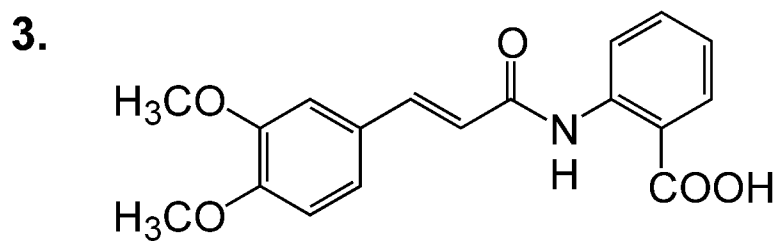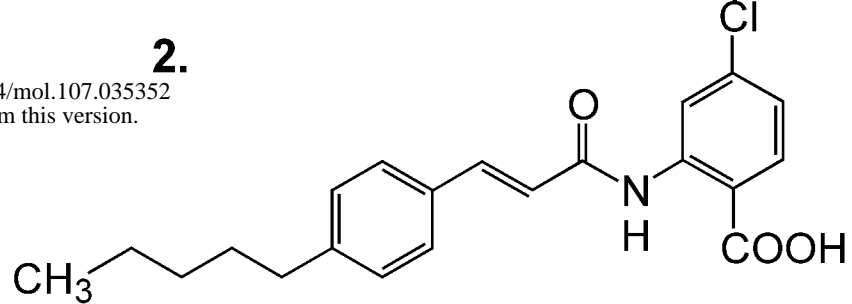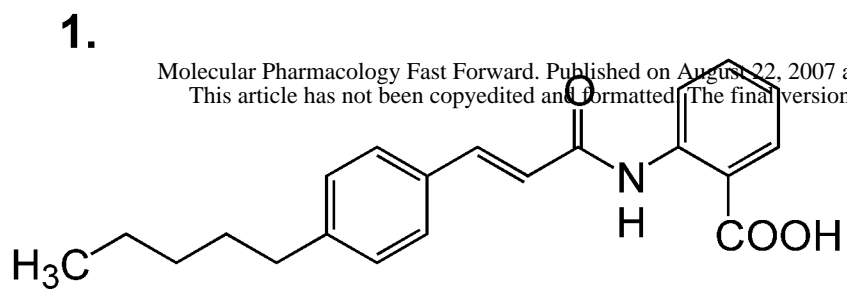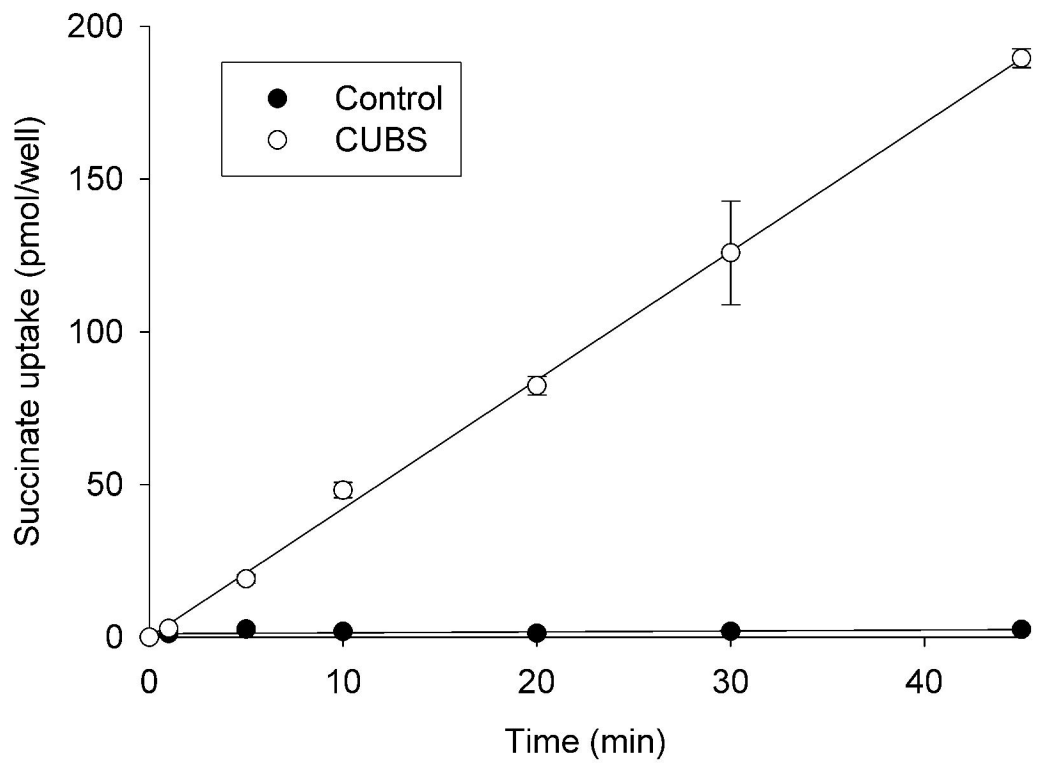
Figure 1

Figure 2

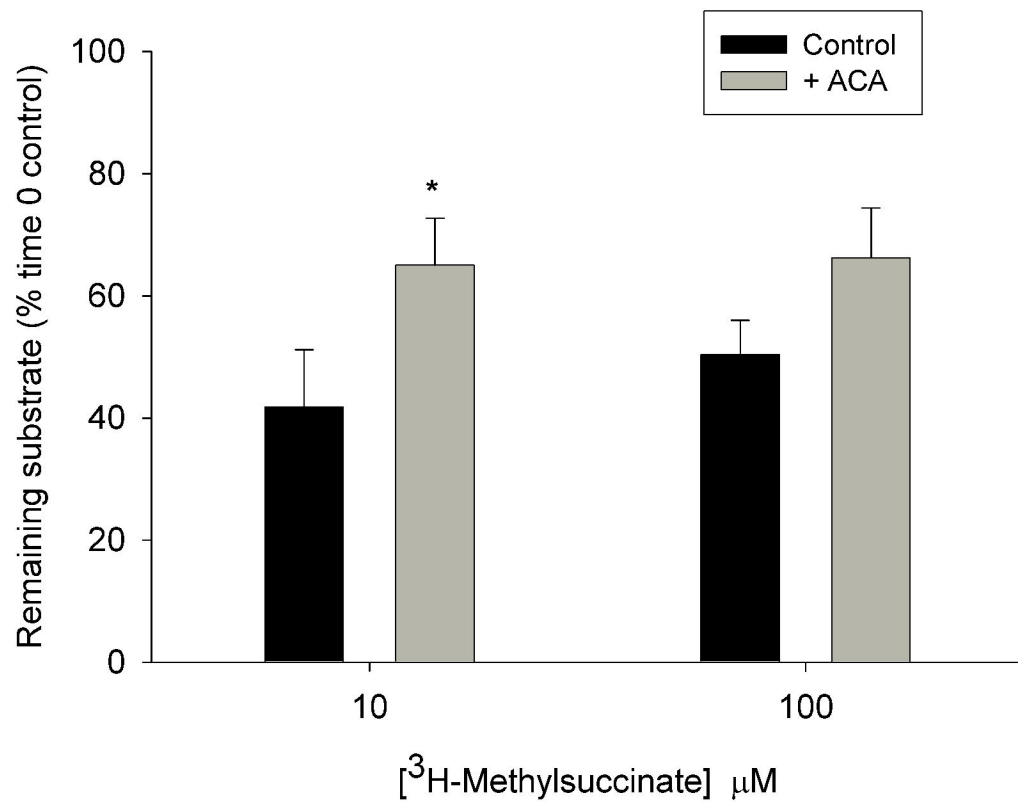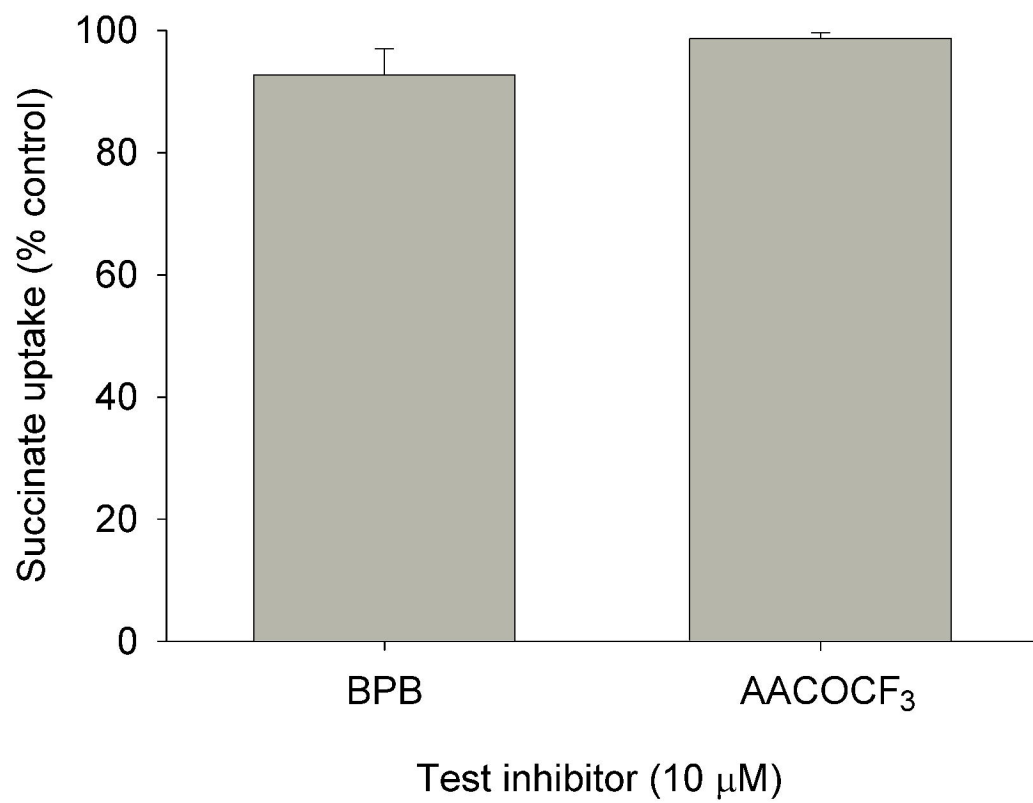Figure 3
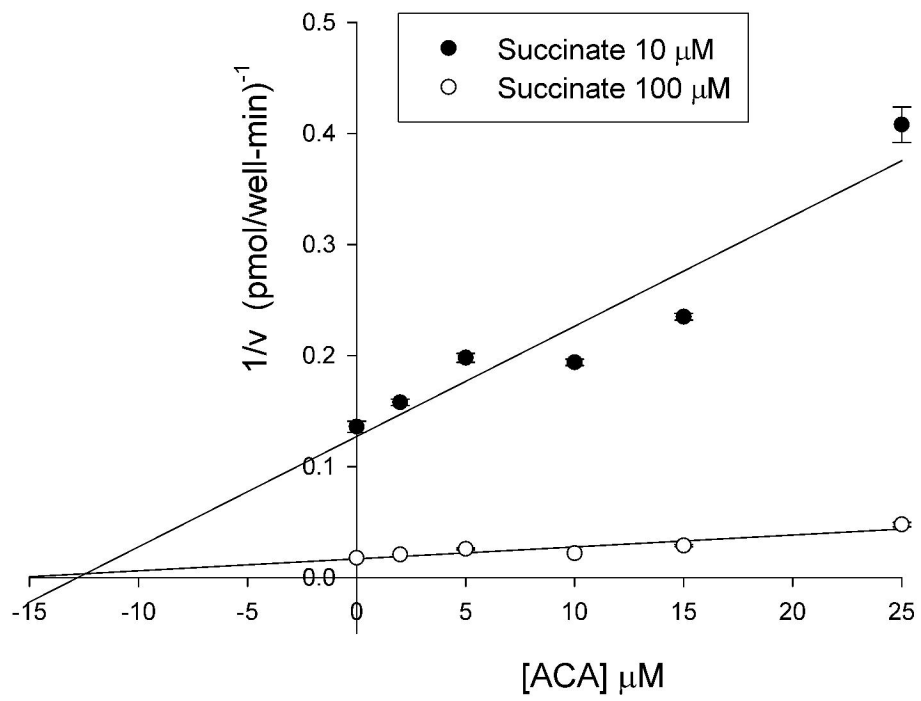
Figure 4
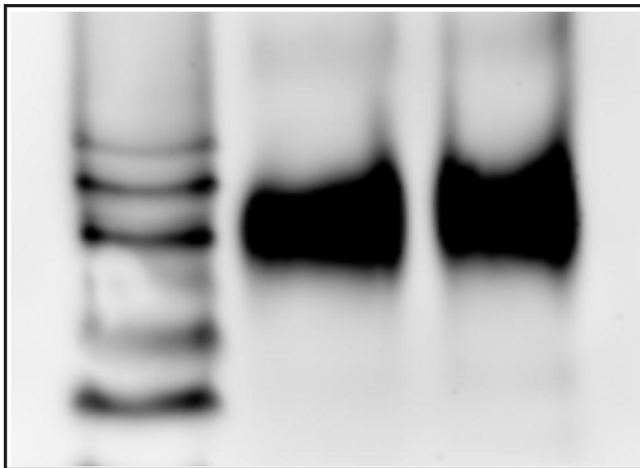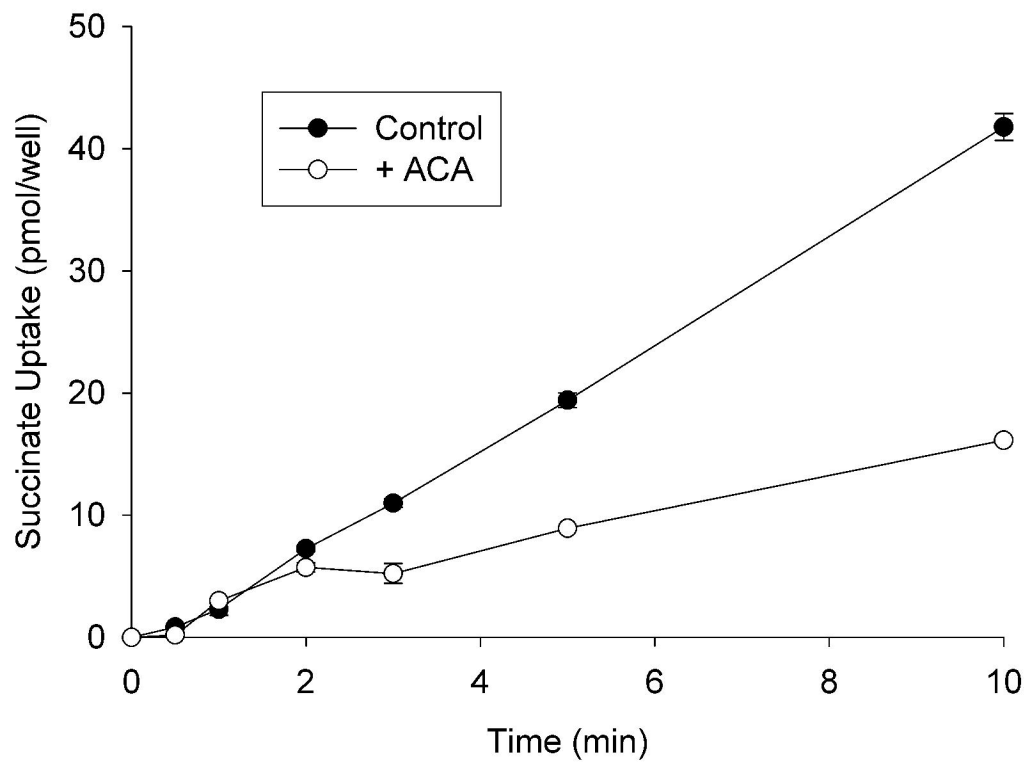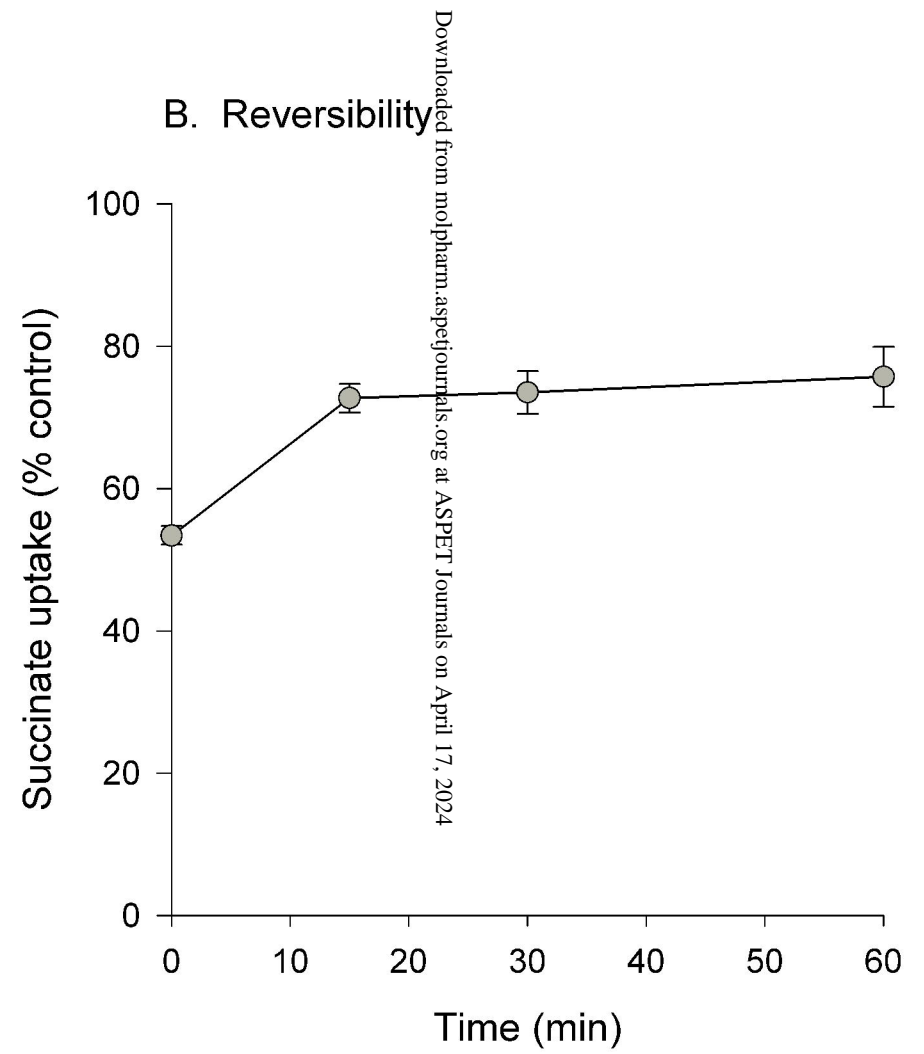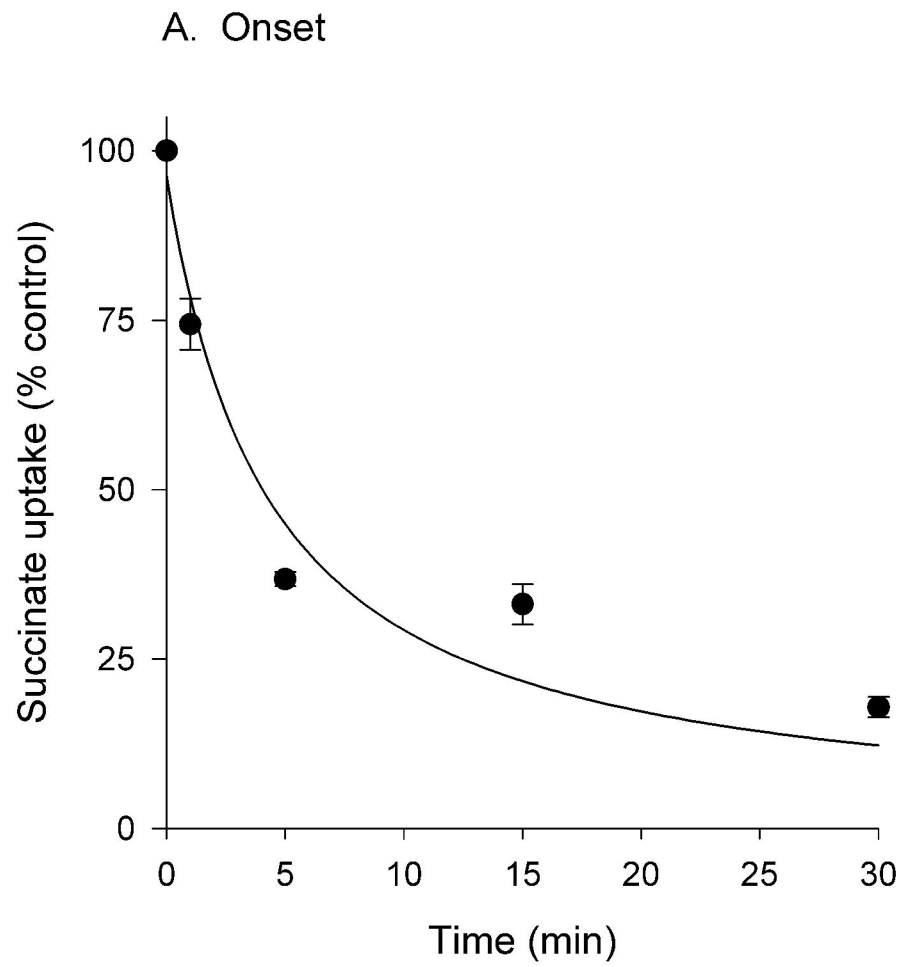
Figure 5

Figure 6

A. Onset

B. Reversibility

Figure 7

Figure 8

Figure 9

Figure 10

Figure 11